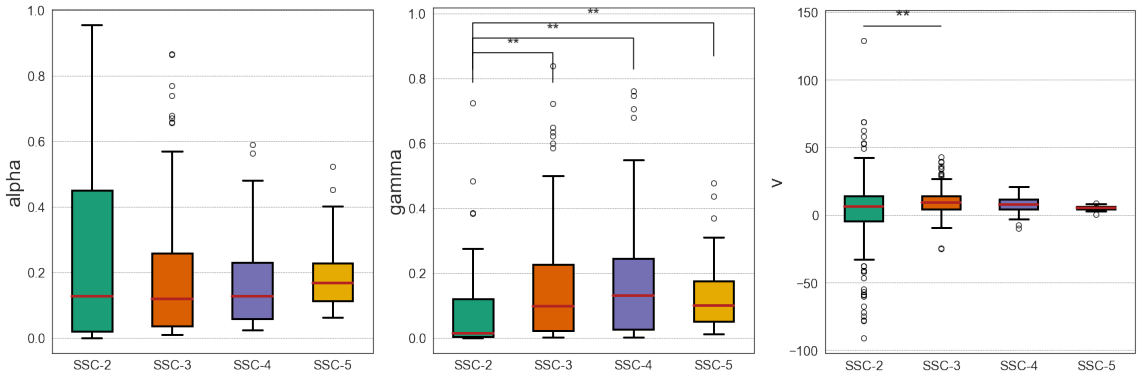

(1) Distribution of α

(2) Distribution of γ

(3) Distribution of v

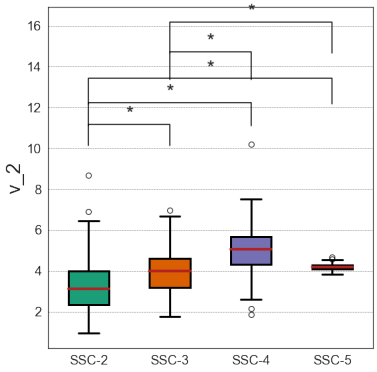

(4) Distribution of v_2

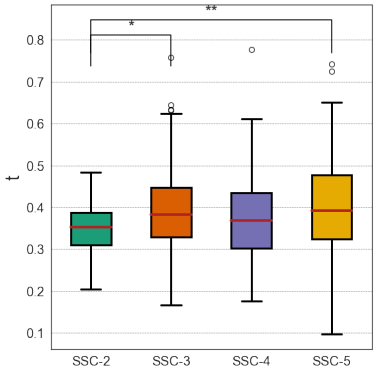

(5) Distribution of t_{res}

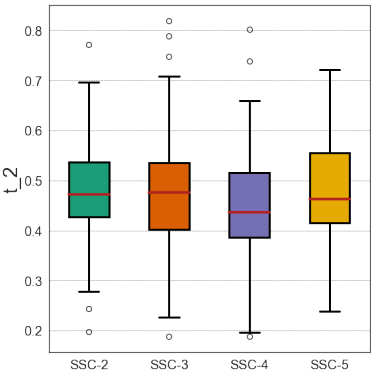

(6) Distribution of ndt_2

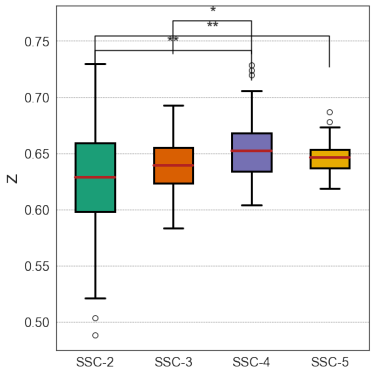

(7) Distribution of z

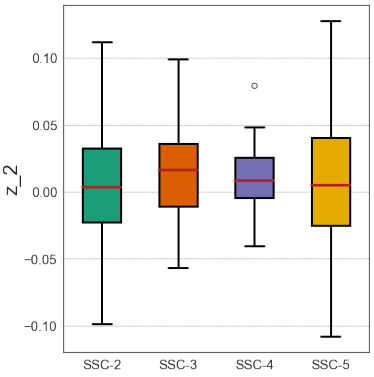

(8) Distribution of z_2

Figure 1: The posterior mean distribution of parameters from the dynamic & hybrid RLDDM. α = learning rate, γ = discount rate, v = first-stage drift rate, v_2 = second-stage drift rate, t_{res} = residual time, ndt_2 = second-stage non-decision time, z = first-stage starting-point bias, z_2 = second-stage starting-point bias. Significant results of pairwise *t*-tests are indicated with asterisks ($* = p < .05, ** = p < .01, *** = p < .001$).

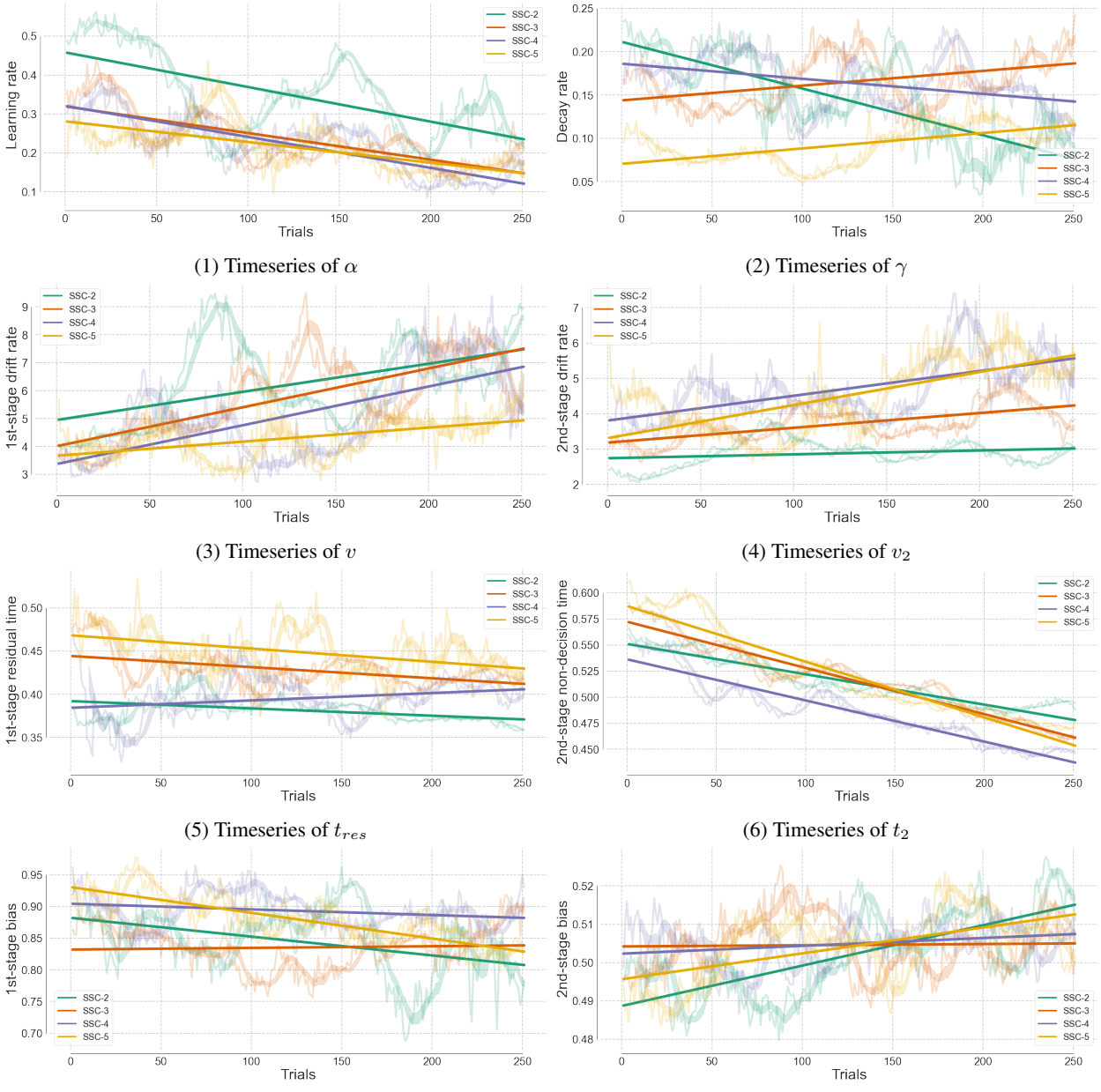

(1) Timeseries of α

(2) Timeseries of γ

(3) Timeseries of v

(4) Timeseries of v_2

(5) Timeseries of t_{res}

(6) Timeseries of t_2

(7) Timeseries of z

(8) Timeseries of z_2

Figure 2: Timeseries of parameters from the dynamic & hybrid RLDDM. α = learning rate, γ = discount rate, v = first-stage drift rate, v_2 = second-stage drift rate, t_{res} = residual time, ndt_2 = second-stage non-decision time, z = first-stage starting-point bias, z_2 = second-stage starting-point bias. Thin lines indicate the mean timeseries of participants, which is overlaid by a rolling average of window=10 represented as thick lines. Straight lines indicate least squares regression lines, and shaded areas represent standard errors.

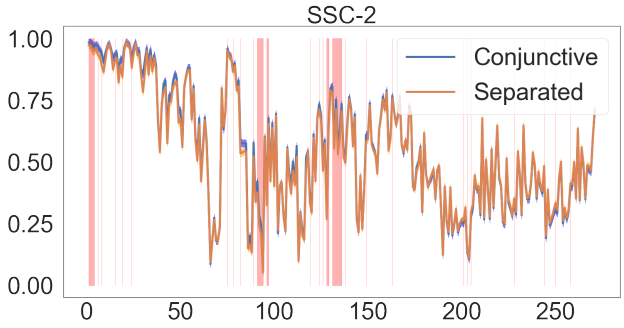

(1) Timeseries of w_{rep} in SSC-2 split into two groups. N=25, N=75 for conjunctive and separated groups, respectively.

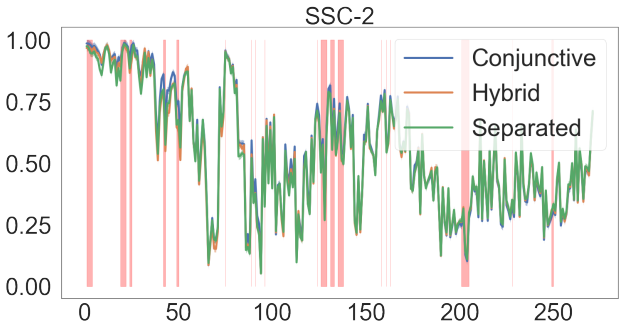

(2) Timeseries of w_{rep} in SSC-2 split into three groups. N=19, N=16, N=65 for conjunctive, hybrid, and separated groups, respectively.

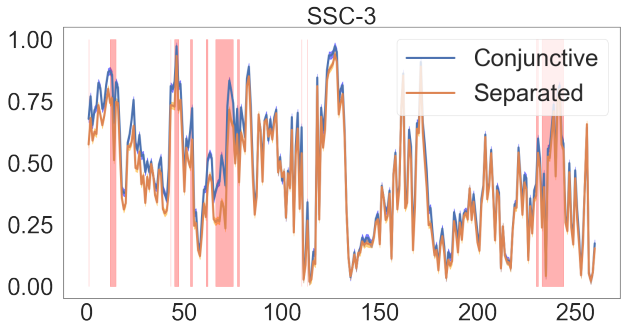

(3) Timeseries of w_{rep} in SSC-3 split into two groups. N=39, N=66 for conjunctive and separated groups, respectively.

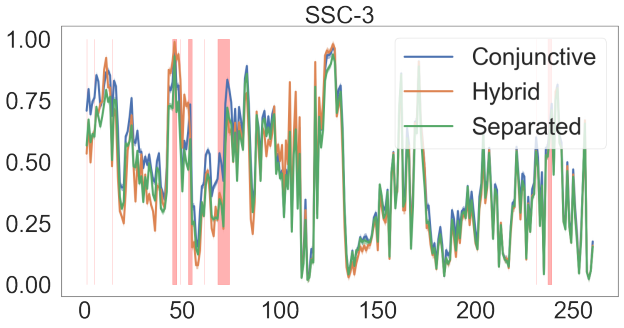

(4) Timeseries of w_{rep} in SSC-3 split into three groups. N=36, N=6, N=63 for conjunctive, hybrid, and separated groups, respectively.

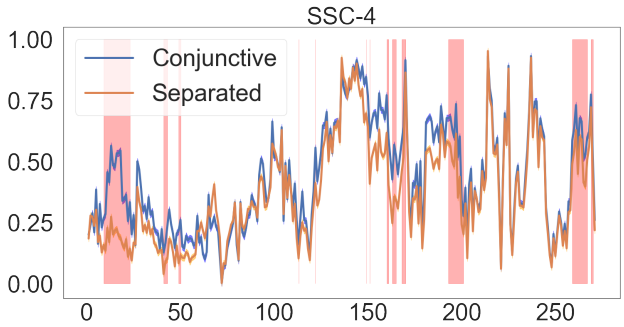

(5) Timeseries of w_{rep} in SSC-4 split into two groups. N=23, N=80 for conjunctive and separated groups, respectively.

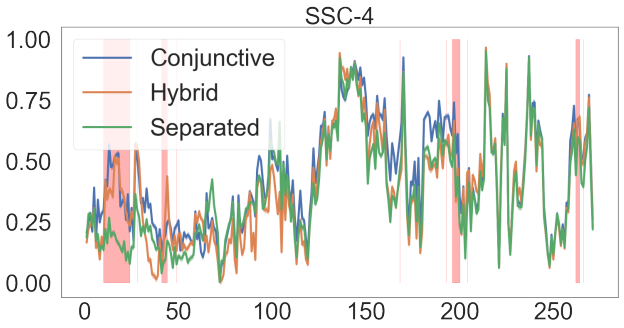

(6) Timeseries of w_{rep} in SSC-2 split into three groups. N=21, N=9, N=73 for conjunctive, hybrid, and separated groups, respectively.

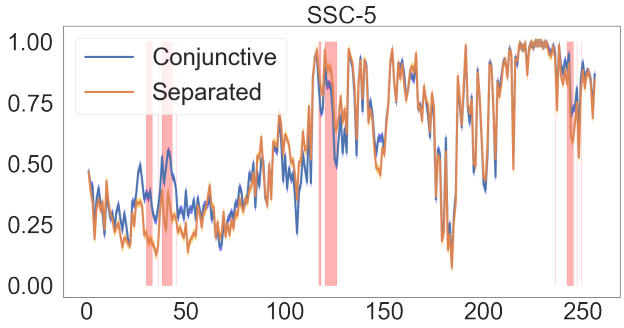

(7) Timeseries of w_{rep} in SSC-5 split into two groups. N=55, N=52 for conjunctive and separated groups, respectively.

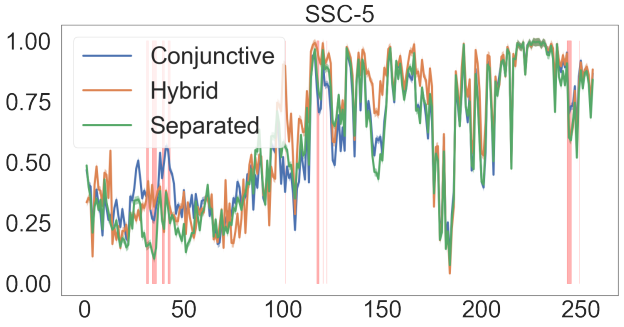

(8) Timeseries of w_{rep} in SSC-2 split into three groups. N=53, N=8, N=46 for conjunctive, hybrid, and separated groups, respectively.

Figure 3: Timeseries of w_{rep} with subjects split into two or three groups, according to their w_{rep} point-estimate. Y-axes indicate w_{rep}, where 1 indicates conjunctive and 0 indicates separated. **(a)** Participants were split into two groups, where subjects $w_{rep} > 0.5$ were labeled as "conjuctive" and $w_{rep} <= 0.5$ were classified as "separated" groups. **(b)** Participants were split into three groups, where subjects $w_{rep} > 0.6$ were labeled as "conjuctive," $0.3 < w_{rep} <= 0.6$ as "hybrid,' and $w_{rep} <= 0.3$ were classified as "separated" groups. Shaded areas indicate windows where there was a significant across-group difference in w_{rep}.

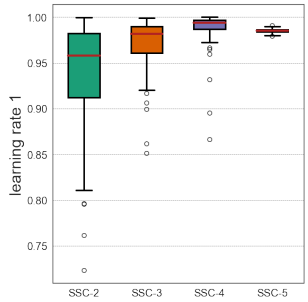

(1) Distribution of learning rate (α).

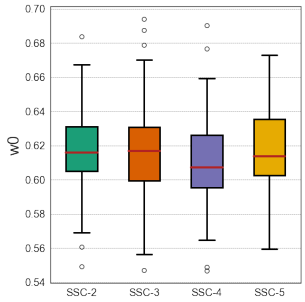

(2) Distribution of the model-based parameter (w).

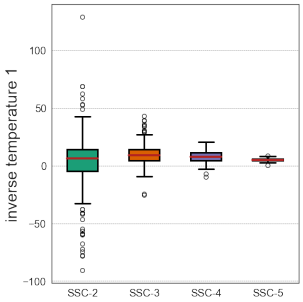

(3) Distribution of the first-stage inverse temperature parameter (β_1).

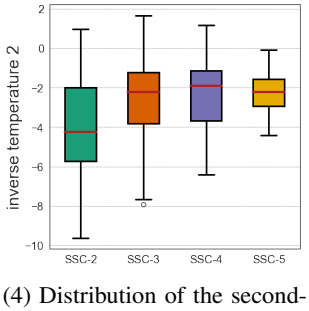

(4) Distribution of the second-stage inverse temperature parameter (β_2).

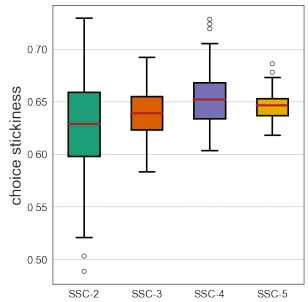

(5) Distribution of the choice-stickiness parameter.

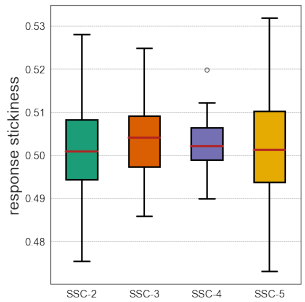

(6) Distribution of the response-stickiness parameter.

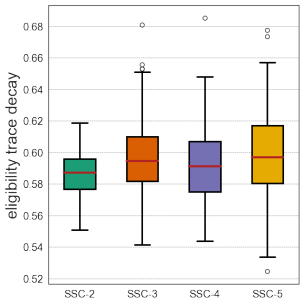

(7) Distribution of the eligibility trace parameter (λ).

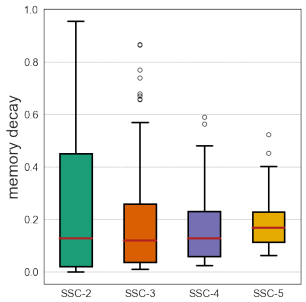

(8) Distribution of the memory decay parameter (γ).

Figure 4: Distribution of the dual-system RL model parameters. Post-hoc t-test (Tukey HSD) of learning rate (α): SSC-2 vs. SSC-3: mean difference=-.11, 95% CI [-.2, -.009], $p = .027$; SSC-2 vs. SSC-4: mean difference=-.11, 95% CI [-.2, -.011], $p = .023$; SSC-2 vs. SSC-5: mean difference=-.11, 95% CI [-.21, -.014], $p = .018$. Post-hoc t-test (Tukey HSD) of eligibility trace (λ): SSC-2 vs. SSC-3: mean difference=-.13, 95% CI [-.255, -.004], $p = .04$; SSC-2 vs. SSC-4: mean difference=-.21, 95% CI [-.33, -.08], $p = .001$; SSC-2 vs. SSC-5: mean difference=-.19, 95% CI [-.32, -.07], $p = .001$. Post-hoc t-test (Tukey HSD) of memory decay (γ): SSC-2 vs. SSC-5: mean difference=-.095, 95% CI [-.17, -.02], $p = .007$.

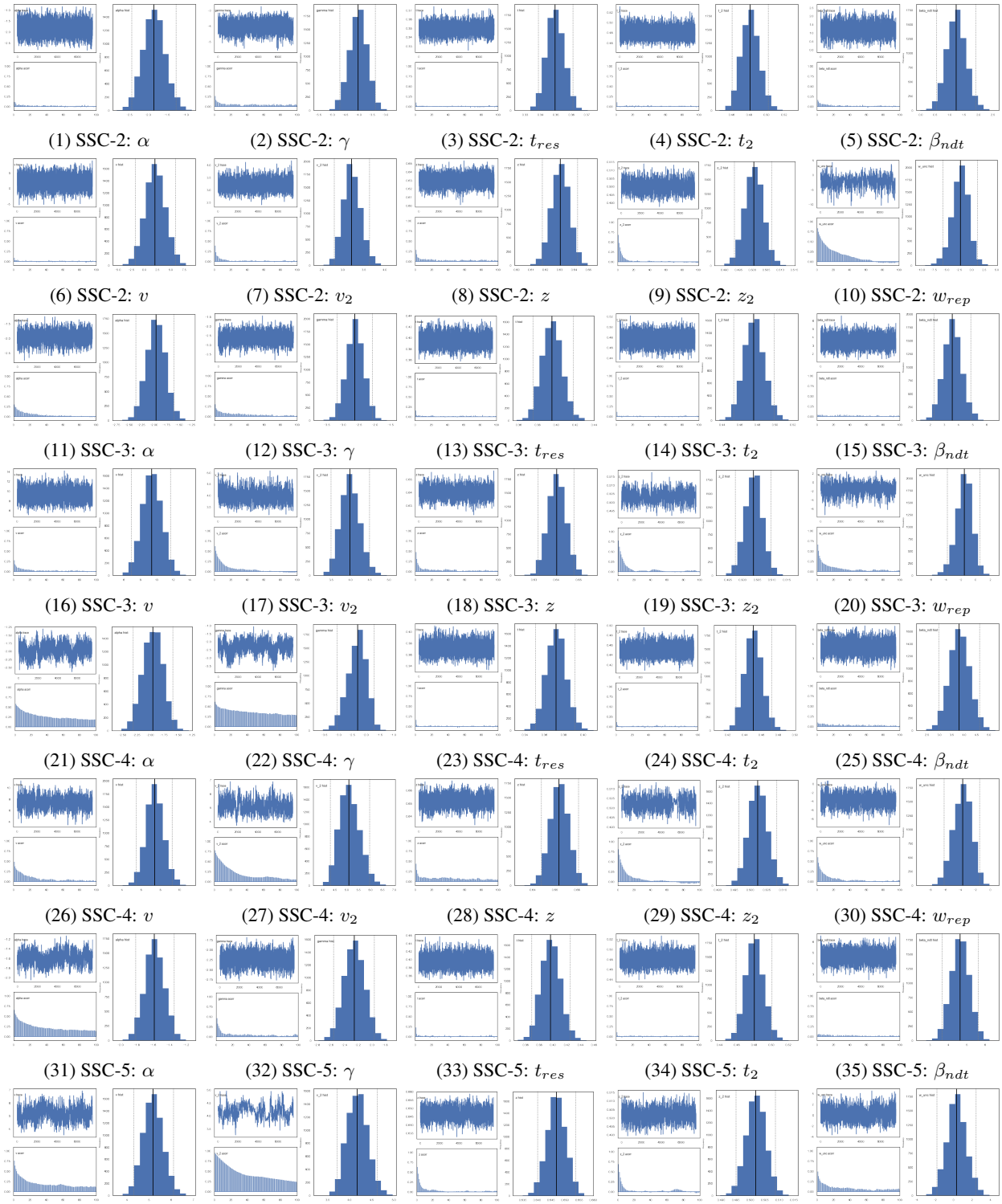

(1) SSC-2: α (2) SSC-2: γ (3) SSC-2: t_{res} (4) SSC-2: t_2 (5) SSC-2: β_{ndt}

(6) SSC-2: v (7) SSC-2: v_2 (8) SSC-2: z (9) SSC-2: z_2 (10) SSC-2: w_{rep}

(11) SSC-3: α (12) SSC-3: γ (13) SSC-3: t_{res} (14) SSC-3: t_2 (15) SSC-3: β_{ndt}

(16) SSC-3: v (17) SSC-3: v_2 (18) SSC-3: z (19) SSC-3: z_2 (20) SSC-3: w_{rep}

(21) SSC-4: α (22) SSC-4: γ (23) SSC-4: t_{res} (24) SSC-4: t_2 (25) SSC-4: β_{ndt}

(26) SSC-4: v (27) SSC-4: v_2 (28) SSC-4: z (29) SSC-4: z_2 (30) SSC-4: w_{rep}

(31) SSC-5: α (32) SSC-5: γ (33) SSC-5: t_{res} (34) SSC-5: t_2 (35) SSC-5: β_{ndt}

(36) SSC-5: v (37) SSC-5: v_2 (38) SSC-5: z (39) SSC-5: z_2 (40) SSC-5: w_{rep}

Figure 5: Visual inspection of convergence in Monte-Carlo Markov Chains for our model (dynamic & hybrid RLDDM). α = learning rate, γ = discount rate, v = first-stage drift rate, v_2 = second-stage drift rate, t_{res} = residual time, ndt_2 = second-stage non-decision time, z = first-stage starting-point bias, z_2 = second-stage starting-point bias. All of the parameters showed strong indication of convergence (e.g., "furry-caterpillar" like posterior distribution, low auto-correlation). Critically, the results of visual inspection matched quantitative metrics (all Gelman-Rubin values < 1.1).

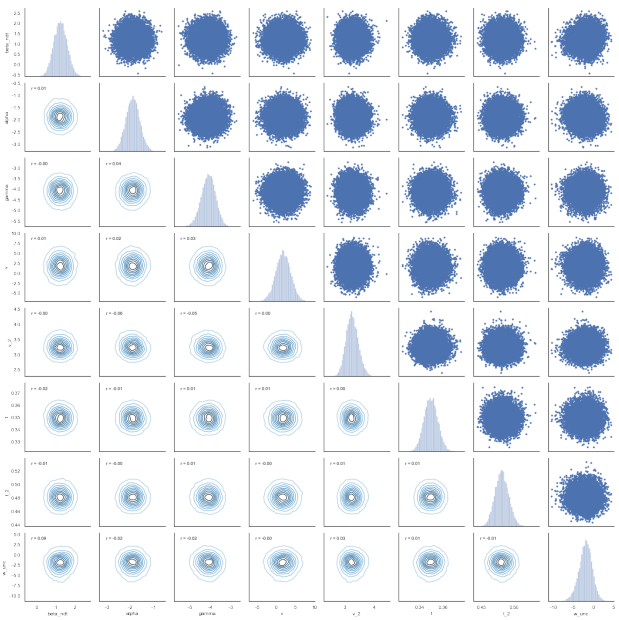

(1) Joint posterior distribution of parameters in SSC-2

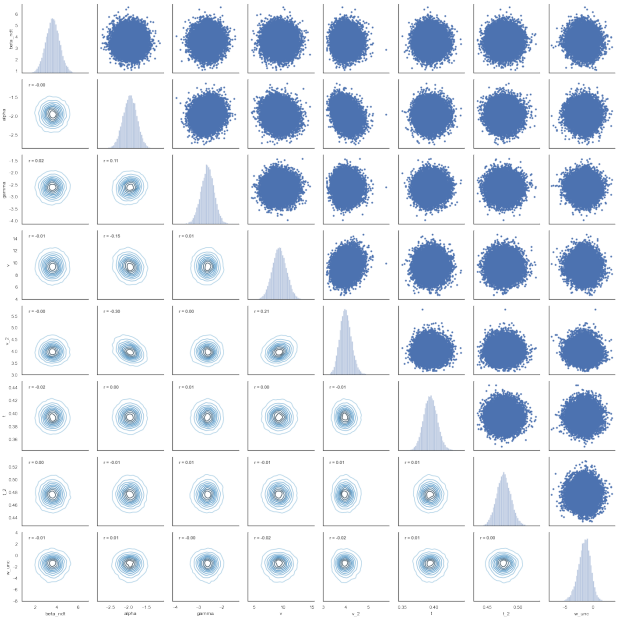

(2) Joint posterior distribution of parameters in SSC-3

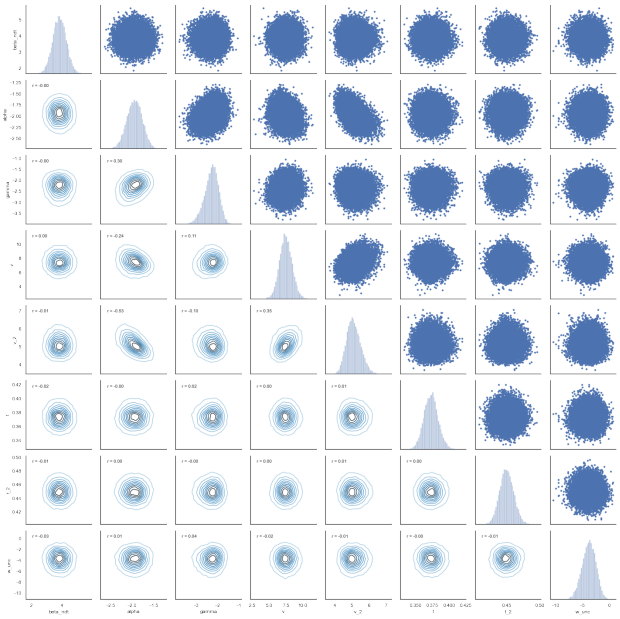

(3) Joint posterior distribution of parameters in SSC-4

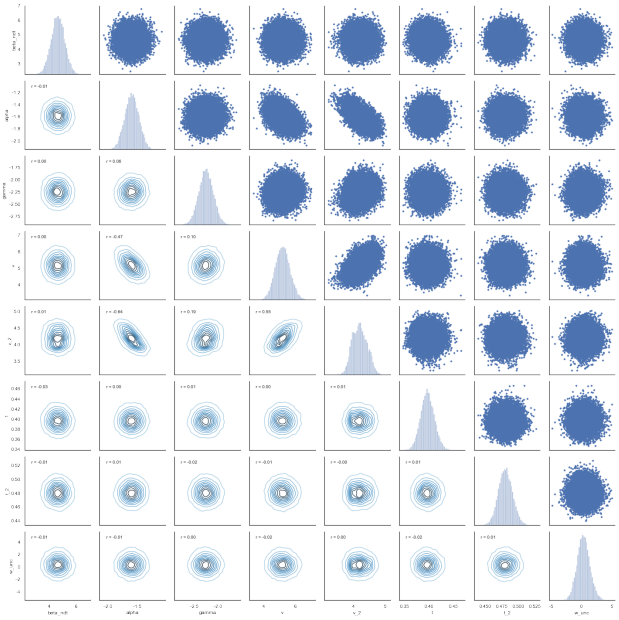

(4) Joint posterior distribution of parameters in SSC-5

Figure 6: Joint posterior distribution of parameters. α = learning rate, γ = discount rate, v = first-stage drift rate, v_2 = second-stage drift rate, t_{res} = residual time, ndt_2 = second-stage non-decision time, z = first-stage starting-point bias, z_2 = second-stage starting-point bias. w_{unc} indicates w_{rep}. No spurious correlations between parameters were found.

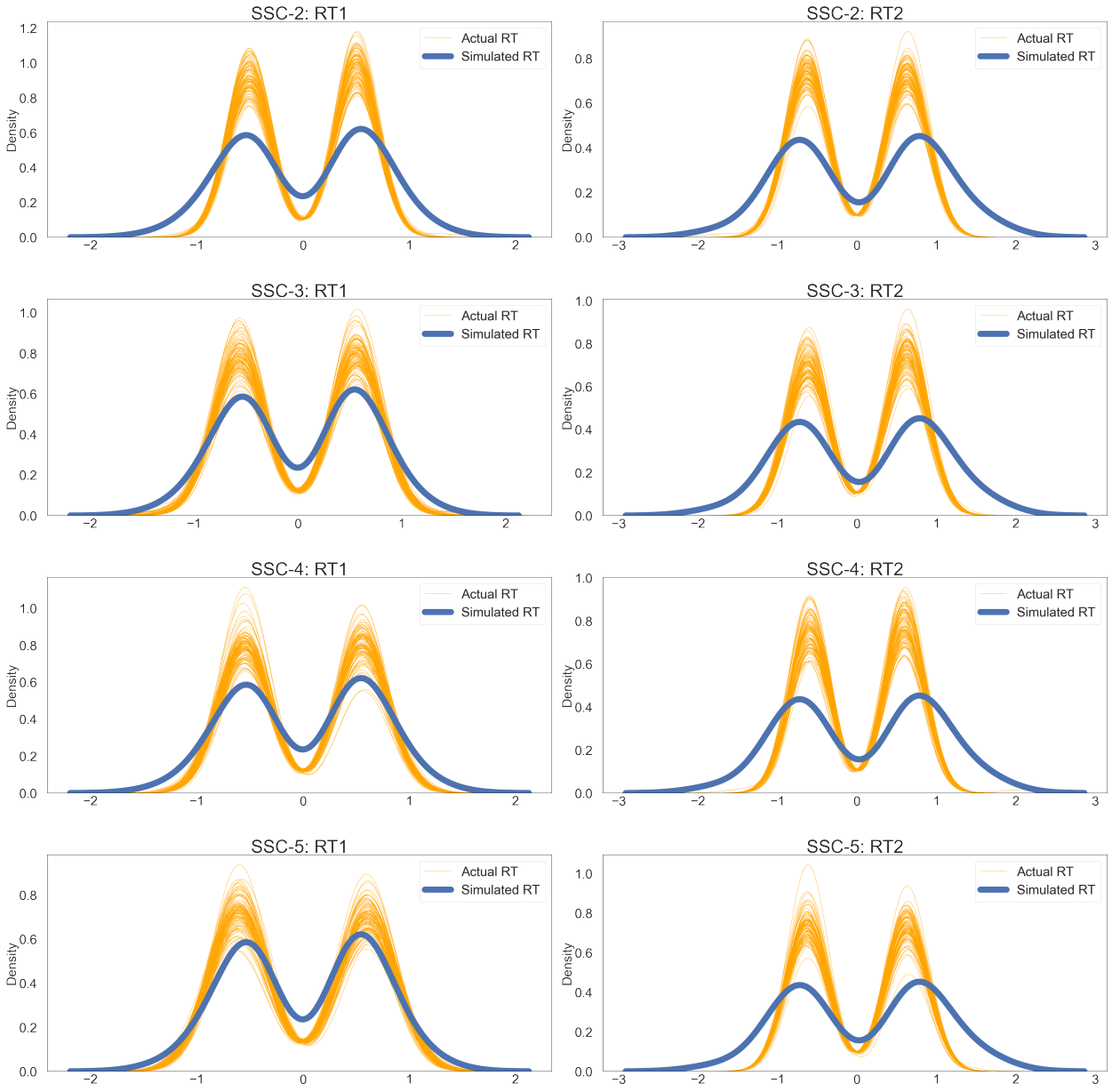

Figure 7: Posterior predictive check by comparing simulated vs. empirical response time data. Simulations were performed by extracting the subject-level parameters from the posterior distribution of the best-fitting model (dynamic & hybrid RLDDM), and 100 simulations were performed for each condition. The yellow line stands for the kernel density estimate of each iteration's distribution, which is overlaid with the distribution of the empirical RT that is represented as the blue line. For differential visualization of upper vs. lower boundaries (left and right choices), RTs were coded in a signed manner according to choice.